Talanta 110 (2013) 39–45

Contents lists available at SciVerse ScienceDirect

Talanta

journal homepage: www.elsevier.com/locate/talanta

Vortex focusing of ions produced in corona discharge

Yuri N. Kolomiets *, Viktor V. Pervukhin

Nikolaev Institute of Inorganic Chemistry of SB RAS, Acad. Lavrentieva Avenue 3, 630090 Novosibirsk, Russia

ARTICLE INFO

Article history:
Received 24 September 2012
Received in revised form
25 January 2013
Accepted 5 February 2013
Available online 14 February 2013

Keywords:
Remote ion sampling
Swirled sampling stream
Atmospheric pressure ion focusing
Corona discharge

ABSTRACT

Completeness of the ion transportation into an analytical path defines the efficiency of ionization analysis techniques. This is of particular importance for atmospheric pressure ionization sources like corona discharge, electrospray, ionization with radioactive (^{3}H, ^{63}Ni) isotopes that produce nonuniform spatial distribution of sample ions. The available methods of sample ion focusing are either efficient at reduced pressure (~1 Torr) or feature high sample losses. This paper deals with experimental research into atmospheric pressure focusing of unipolar (positive) ions using a highly swirled air stream with a well-defined vortex core. Effects of electrical fields from corona needle and inlet capillary of mass spectrometer on collection efficiency is considered. We used a corona discharge to produce an ionized unipolar sample. It is shown experimentally that with an electrical field barrier efficient transportation and focusing of an ionized sample are possible only when a metal plate restricting the stream and provided with an opening covered with a grid is used. This gives a five-fold increase of the transportation efficiency. It is shown that the electric field barrier in the vortex sampling region reduces the efficiency of remote ionized sample transportation two times. The difference in the efficiency of light ion focusing observed may be explained by a high mobility and a significant effect of the electric field barrier upon them. It is possible to conclude based on the experimental data that the presence of the field barrier narrows considerably (more than by one and half) the region of the vortex sample ion focusing.

1. Introduction

The advance of research with the methods using mass-spectrometry with the atmospheric pressure ionization (electrospray, atmospheric pressure chemical ionization, ionization with a radioactive source, AP MALDI etc.) depends to a great extent on the completeness of ion transport into the analytical path. This requires sample ionization near a sampling opening (or capillary) of the mass-spectrometer to avoid diffusion ion losses. Insufficient signal from diffusion ion sources is an old restriction on the experimental application of analytical methods [1]. For these reasons, the development of atmospheric pressure ion focusing techniques is of primary importance since it allows one to move the ionization region aside from the sampling opening and reduce ion losses upon their transportation into the analytical path of the mass-spectrometer.

It should be mentioned that the atmospheric pressure ion focusing is not an easy task, since the classical methods of ions focusing and collimation with electrical and magnetic fields give up in efficiency as the ambient pressure increases. Nevertheless, Kremer et al. [2] have suggested using a conical lens produced by the circular-type floating electrodes for the atmospheric pressure ion collimation. As compared to pull potential, ion losses have decreased and the quality of focusing has improved. But for the floating electrostatic lens to achieve the operating potential a definite period is required during which considerable sample losses are unavoidable.

The use of radio frequency potentials allows increasing pressure upon ion focusing. This is described by Shaffer et al. [3,4], Kim et al. [5] and Clowers et al. [6] where a so called electrodynamic ion funnel is studied. This device represents a system of electrodes as a cone to which a combination of radio frequency (700 kHz) and electric static fields has been applied and which has shown efficient operation under pressures of some tens of Torr offering an increase in ion signal of several orders of magnitude. But the available technology does not allow using this system under pressures near to atmospheric one.

High-field asymmetric waveform ion mobility spectrometry (FAIMS) gives another way for using a combination of radio frequency and electric static fields for the atmospheric pressure ion focusing. For example, for the atmospheric pressure ion transportation from a source to an analyzer Guevremont et al. [7,8] and Barnett et al. [9] used a channel with a gas flow where ion focusing upon their transportation was executed by a

* Corresponding author. Tel.: +7 383 330 95 15; fax: +7 383 330 94 89.
E-mail addresses: ykolom@niic.nsc.ru, ykolom@ngs.ru (Y.N. Kolomiets).

0039-9140/$ - see front matter © 2013 Elsevier B.V. All rights reserved.
http://dx.doi.org/10.1016/j.talanta.2013.02.016

combination of radio frequency and constant electric fields normal to the gas flow. Periodic alternating asymmetric waveform field with the gradient directed along the field force lines was required for ion focusing. This approach can reduce ion losses by more than an order of magnitude, but focusing is not for all ion types, and adjustment of the focusing electric fields in the device depends on ion types and is done for each ion separately.

Owing to the great impact of the laws of gas dynamics on ions under atmospheric pressure, it seems obvious to use gas flows of special configuration for ion focusing. This approach is described in [10–13], where an air amplifier known as a Venturi device was used for ion focusing. This device creates a converging high-speed concentric gas flow around an electrospray tip reducing diffusion of an electrospray pen, facilitating ion desolvation and increasing ion current towards the sampling opening of the MS. Voltage applied to the air amplifier enhances focusing and increases ion current. It should be mentioned that this device has been used for electrospray ionization alone setting all other atmospheric ionization methods aside.

In this paper we discuss focusing ions using a highly swirled air stream together with an additional flow that forms a well-defined vortex core in the swirled stream. Gas dynamic studies [14,15] show that in the swirled stream – with a high swirl intensity owing to a centrifugal stream spread – static pressure in the entire volume is below the external atmosphere, and near the axis a counter flow is produced which radial flow velocity is directed towards its axis. We have shown in [16,17] that a vortex sampling stream as a composite vortex is alone in its ability to focus sample on the axis of the sampling flow at the center of the vortex core thus preventing sample diffusion along the entire counter flow. In [18,19] we described focusing of an ionized bipolar sample with a highly swirled vortex stream released experimentally in spite of a significant effect of recombination processes. The paper suggested deals with an experimental research into unipolar (positive) ion focusing produced in a corona discharge under the action of electric fields of a corona needle and an inlet capillary of a mass-spectrometer.

2. Experimental

Schematic diagram of an experimental unit used is given in Fig. 1. The unit includes a device for vortex ion focusing, a source of ions produced in corona discharge and a mass-spectrometric ion detector.

2.1. Atmospheric pressure vortex ion focusing

This device is described in detail in [19]. We will give a brief device description. Vortex forming air flow, Q_{vortex}, is fed by a centrifugal pump (not shown in Fig. 1) to fixed impeller (1) with an angle of blade 45° and creates a fan vortex stream that spreads over the inside surface of reflector (2) producing a volumetric swirled flow with an axial counter flow along the reflector axis towards the ion source. A value of vortex forming flow, Q_{vortex} was varied in the range from 0 to 9000 ml/s. We used a Disa 55M System Constant-temperature Anemometer of Disa Elektronik A/S, Denmark to calibrate the flow measuring the linear vortex flow rate in the inlet nozzle with a precision of ± 0.02 m/s. We used laboratory air (temperature, 22 °C and relative humidity, 54%) to create the vortex forming flow Q_{vortex}. It might be better to use noble or pure gasses for this purpose, but the high gas flow rates required for the vortex flow creation make this impossible (both due to the cost of experiment and serviceability).

We used an MS sampling capillary (6) to collect ions from the counter flow. It is shown in [17] that for the expressed vortex core

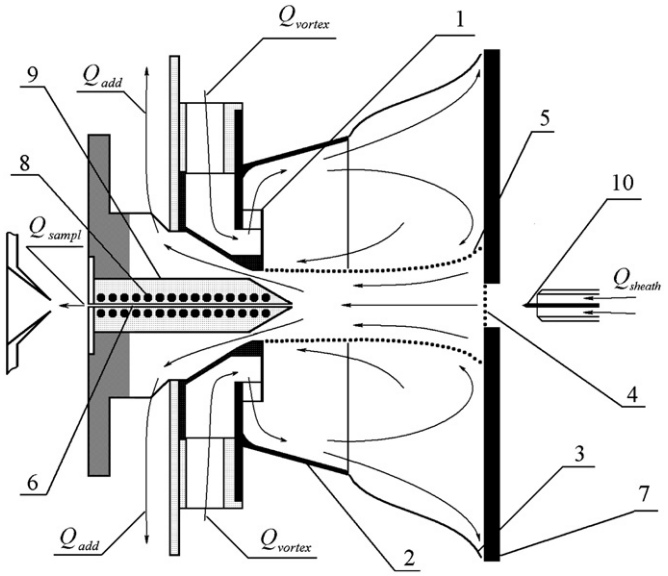

Fig. 1. Schematic diagram of the device for the atmospheric pressure vortex ion focusing for a mass-spectrometer. 1—fixed impeller; 2—reflector; 3—external vortex flow boundary; 4—opening in a plate covered with a metal grid; 5—vortex core boundary; 6—MS sampling capillary; 7—metal plate; 8—sampling capillary heater; 9—housing; and 10—corona needle. Arrows show the direction of gas flows. Values of, Q_{vortex}, Q_{add}, Q_{sampl} and Q_{sheath} are given in the text.

to produce in the counter flow the vortex and sampling flows should be comparable in value, more exactly, their relation Q_{vortex}/Q_{sampl} should be about 1.3. Since the MS sampling flow is very low ($Q_{sampl} \approx 19$ ml/s), a focusing gaseous detector is provided with additional flow, Q_{add}, enveloping coaxially the MS sampling capillary (Fig. 1). This flow helps to create a vortex sampling stream as a composite vortex capable of focusing ions on the sampling flow axis in the center of the vortex core thus preventing ion diffusion along the entire counter flow. It should be mentioned therewith that a surface on which the vortex flow is directed is required to produce a vortex core. For such a surface we used metal plate (7) 250×180 mm^2 in size provided with an opening (4) in the center 10 mm in diameter with a corona needle behind it. We placed the plate together with the corona discharge ion source on an *x*,*y*,*z*-manipulator permitting plate setting in a required position.

In Fig. 1 the external boundary of the swirled flow and vortex core is given by solid lines (3) and dashed lines (5), respectively. The vortex stream reduces the axial pressure by some tens of Pa below the external asmosphere [17], so that ions produced in the corona discharge are pulled through the opening behind the plate into the counter flow region, focused by the vortex core and transported to the inlet opening of the MS sampling capillary.

2.2. Corona discharge

To generate the corona discharge we used needle (10) positioned behind the plate to which we applied a high voltage of (+5 kV) from a BPV-5 DC power source (0.3–8 kV, 400 mcA, Ltd. "High-voltage Technologies", Moscow, Russia). As a counter electrode we used plate (7) of the vortex forming device which potential as well as the potential of all the device components was at the earth potential. We left an opening (4) in the center of the plate either open or covered with a grid from 12H18N10T stainless steel, GOST 3826-82 with a mesh size of 0.3×0.3 mm^2 and a wire diameter of 0.12 mm (grid 1), and with a mesh size of 0.094×0.094 mm^2 and a wire diameter of 0.055 mm (Ltd. "Torgovyj Dom Setok", Moscow, Russia). As shown in [20], an

opening in the plate disrupts the structure of the composite vortex decreasing considerably reduced the pressure inside the vortex core. Hence, the grids covering the opening reduced the disruption of the structure of the swirled sampling stream and reduction of its focusing action.

In our experiment ions are produced behind the plate. Electric field of the needle (with no grid) and reduced pressure of the sampling vortex flow itself pull ions through the opening into the region of the vortex stream counter flow. We used a weak sheath flow, Q_{sheath}, (0–200 ml/s) enveloping coaxially corona needle (10) to enhance ions pull through the opening. It is also important to study the action of flow, Q_{sheath}, from the perspective of the applicability of the vortex focusing for electrospray sample ionization, since the same structure of a gas flow is used in some electrospray ionization sources [21].

2.3. Mass-spectrometric ion detector

As a mass-spectrometric detector we used a mass-spectrometer with atmospheric pressure ionization developed on the basis of an MX-7304 mass-analyzer described in [22]. We modified the detector to use it with the system of vortex ion focusing. We replaced a sampling nozzle by steel capillary (6) 0.3 mm in I.D., 2 mm in O.D. and 100 mm in length. With heater (8) we heated the capillary to a temperature of 150 °C. We controlled temperature with a copper–constantan thermocouple positioned at the outer surface of the capillary. The heater was covered with housing (9) 16 mm in diameter provided with a stainless steel cone with an angle of 60°. We placed the cone tip in an additional flow channel (20 mm in diameter) so that the inlet capillary opening was in the region of the vortex stream counter flow. The cone housing provided a streamline motion of additional flow, Q_{add}, around the sampling capillary.

For positive ion analysis, the design of the mass-analyzer used assumes the existence of positive voltage to ground at the sampling capillary. In our experiments the voltage at the capillary was 130 V, which corresponded to the maximum device sensitivity. This voltage at the capillary (housing) creates a barrier for ion transportation into the capillary. In this paper we investigate a possibility of overcoming this barrier with a vortex focusing. Table 1 gives the main parameters of the experimental device.

2.4. Chemicals

We tested protonated ion focusing of *diethylamine*—$HN(C_2H_5)_2$ (molecular weight, 73), *aniline*—$H_2NC_6H_5$ (molecular weight, 93), *N,N-diethylacetamid*—$CH_3CON(C_2H_5)_2$ (molecular weight, 115) and *triamylamine*—$N(C_5H_{11})_3$ (molecular weight, 227). We subjected substances to equilibrium distillation before usage to remove oxides.

It should be mentioned that we chose substances with a more than a 3-fold mass spread for studies to reveal a possible difference in vortex focusing of ions with a different molecular weight.

3. Results and discussion

As mentioned in Section 1, the paper deals with research into the positive ion vortex focusing for mass-spectrometry under the action of electric fields of the corona needle and MS inlet capillary. The electric field exposure, especially from the high-voltage corona needle potential, can significantly affect the processes of ion focusing with a gas flow. This effect is especially important when the plate is missing, or the opening in the plate is not covered with the grid. The results obtained may be grouped in three parts.

Table 1
Main parameters of the experimental device.

Parameter	Value
System of vortex ion focusing	
Reflector diameter, D_R (mm)	100
Diameter of fixed vortex impeller (mm)	58
Width of fixed vortex impeller (mm)	5
Diameter of additional channel (mm)	21
Vortex flow, Q_{vortex} (cm^3/s)	0–9600
Additional flow, Q_{add} (cm^3/s)	0–3800
Plate dimensions (mm^2)	250×180
Diameter of plate opening for ion removal (mm)	10
Corona discharge	
Voltage (kV)	5
Current (μA)	50
Distance from needle to screen (mm)	5
Grid 1, mesh size (mm^2), wire diameter (mm)	0.3×0.3, 0.12
Grid 2, mesh size (mm^2), wire diameter (mm)	0.094×0.094, 0.055
Range of sheath flow, Q_{sheath} (cm^3/s)	0–200
Diameter of sheath channel, (mm)	5
Ion detector	
Inside diameter of sampling capillary (mm)	0.3
Length of sampling capillary (mm)	100
Sampling capillary temperature (°C)	150
Flow through sampling capillary, Q_{sampl} (ml/s)	≈ 19
Housing diameter (mm)	16
Cone angle (deg.)	60
Voltage at housing and sampling capillary (V)	130

The first part of the result deals with research into the impact of electric fields of the corona needle and the MS inlet capillary on the vortex focusing of positive ions of different compounds. To evaluate this impact, we used the dependence of the MS signal on vortex $I(Q_{vortex})$, and additional, $I(Q_{add})$, flows with different designs of the vortex forming devices: with no plate, the plate with uncovered opening, the plate with an opening covered with a grid. The research results permit choosing an optimal design of the vortex forming device and operating values of Q_{vortex} and Q_{add} for subsequent experiments.

The second part deals with research into the remote efficiency of the vortex stream upon positive ion sampling. To do this, we determined the dependence of registered signal, I, on distance, L, between the reflector and plate of the vortex forming device. From the research results we determined operating distances to test the efficiency of the ionized sample collection with the vortex stream.

The third part describes an investigation of the efficiency of the ionized sample positive ion collection with the vortex stream. To do this, we determined the dependence of signal, I, on the value of the ionization source displacement from the sampler axis.

3.1. Determination of the optimal design of the vortex forming device and operating values of vortex and additional flows

We have tested vortex forming devices of three designs as follows: with no plate, the plate with uncovered opening, and the plate with the opening covered with the grid. All three device designs differ both in electric field distribution and gas-dynamic behavior. We used an ELCUT software (Ltd. "Tor", 22, Moskovskii pr., Litt. T, room 5H, 190013, Saint-Petersburg, Russia) to calculate electric field going from the device design and potentials of the corona needle and sampling capillary. To evaluate gas-dynamic structure, we measured reduced pressure at the axis of the vortex forming device using an inclined U-shape alcohol manometer with an angle of 10°. Fig. 2 gives the curve of *Ez* component of the electric field intensity versus the distance along the sampler axis for different designs of the vortex forming device.

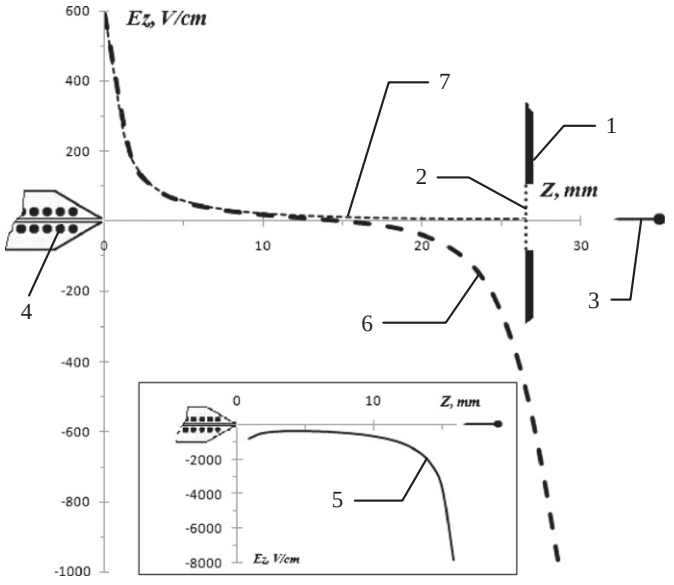

Fig. 2. Curve of the electric field intensity versus distance for different designs of the vortex forming device. 1—plate, 2—grid, 3—corona needle, 4—MS inlet capillary, 5—with no plate, 6—plate without grid, 7—plate with grid, *Ez* component of electric field along the *Z*-axis, and *z* distance from MS capillary opening along the *Z*-axis.

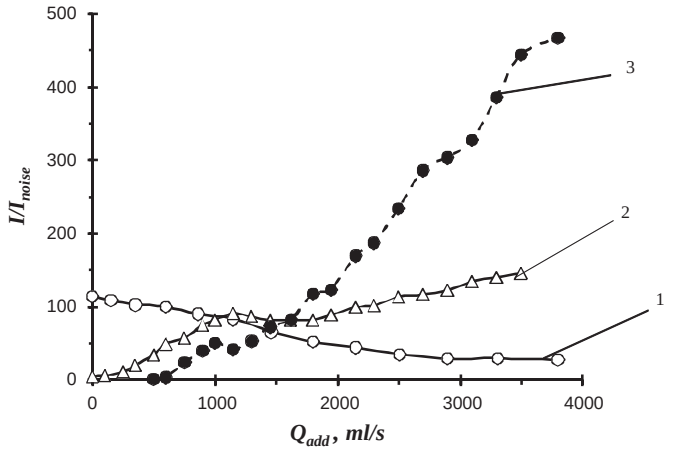

Fig. 3. Curve of the total MS ion current versus additional flow for different vortex forming device designs. 1—with no plate, 2—plate without grid, and 3—plate with grid. Vortex flow, Q_{vortex}=9000 ml/s, L=10 mm.

As Fig. 2 suggests electric field, with no plate (inset at the bottom of Fig. 2), is negative and directed from the needle to the inlet capillary. Under the action of the field a portion of positive sample ions next to the sampler axis is transported from the needle to the inlet opening of the MS sampling capillary, trapped by low sampling flow, Q_{sampl}, and fed through the capillary to the MS for detection. The maximum ion current of the MS – with this vortex forming device design – is registered with no flows when $Q_{vortex}=Q_{add}=0$. When any of the flows is fed, a reduction of the MS signal is registered.

Fig. 3 gives the curve of the total MS ion current versus additional flow, Q_{add}, for different vortex forming device designs with a maximum vortex flow, Q_{vortex}=9000 ml/s. With no plate (Fig. 3, curve 1) the MS signal reduces as the additional flow increases to a maximum value of Q_{add}=3800 ml/s, which should be attributed to the increasing sample losses due to a low efficiency of ion collection with the vortex flow. Indeed, the swirled sampling flow with no plate represents a forced vortex with unformed core. Such a flow features a low reduced pressure (27 Pa, Table 2) and a radial velocity that is three times less than the counter flow velocity [23]. As a result of the counter flow ion transportation from the source to the inlet MS capillary most of ions do not reach the region where the sample is trapped by sampling flow, Q_{sampl}, and are lost for analysis escaping with additional and vortex flows. Both field and gas-dynamic conditions change as the plate is introduced. The null metal plate (when the opening is not covered with the grid), the electric field of the needle, and the opposed field of the inlet MS capillary transporting positive sample ions from the inlet capillary to the plate begins to affect the motion of ions. For the plate without the grid, electric field near the inlet capillary is positive, creates a field barrier for positive ions and becomes negative at a distance of 15 mm (Fig. 2, curve 6). For the plate with the grid, the barrier is created as far as the plate (Fig. 2, curve 7). As a result the MS signal – with a zero additional flow – is either missing (plate with the grid, Fig. 3, curve 3) or is very low (plate without the grid, Fig. 3, curve 2). The signal for the plate without the grid is likely to derive from the fact that a portion of ions is fed by the needle field into the region where they are first trapped by the counter vortex flow and then by sampling flow, Q_{sampl}. The MS signal for the device design with the plate increases with additional flow, Q_{add}, as the efficiency of the vortex stream focusing enhances. An increase in the efficiency of ion focusing for the plate with the grid is the most evident for the values of Q_{add} above 1500 ml/s. With Q_{add}=3800 ml/s the MS signal is five times greater than the maximum MS signal when no plate is used. Such a significant effect of the ionized sample focusing for the plate with a grid design results from the formation of an expressed vortex core in the vortex flow. The value of reduced pressure at the stream axis is testified equally to the formation of the vortex core. The value of reduced pressure for the plate with the grid is maximum for all the considered designs and reaches the value of 145 Pa (Table 2). The highly reduced pressure pulls sample ions through the grid, and the high radial component of the vortex core velocity collects the sample towards the sampler axis where it is transported to the MS sampling capillary and trapped by sampling flow, Q_{sampl}. The experiment has shown that the vortex forming device design using the plate with the grid turns to be the most efficient for focusing the ionized sample from the corona discharge. We used this device design in subsequent experiments.

Since humid air is used to create the vortex flow, ion-molecular reactions like the charge exchange or clustering may take place between positive ions produced in the corona discharge and air. The vortex flow used for the remote ion sampling increases the time of their transportation from the source to the mass-spectrometer and may affect the intensity and type of the resulting mass-spectrum. But we have not observed qualitative changes in mass-spectra obtained with the vortex sampling or without it. Qualitative changes were not found in mass-spectra registered for the plate positioned at different distances from the sampling opening of mass-spectrometer. Most likely ion-molecular reactions attain equilibrium near the corona needle, and a further increase of time does not affect the type of mass-

Table 2
Reduced pressure at the vortex forming device axis for different device designs. Distance from reflector to the plate, 20 mm. Q_{vortex}=9000 ml/s, Q_{add}=3800 ml/s.

	No plate	Plate with uncovered opening	Plate with grid 1	Plate with grid 2
Reduced pressure $\lvert(P-P_{atm})\rvert$ (Pa)	27	104	131	145

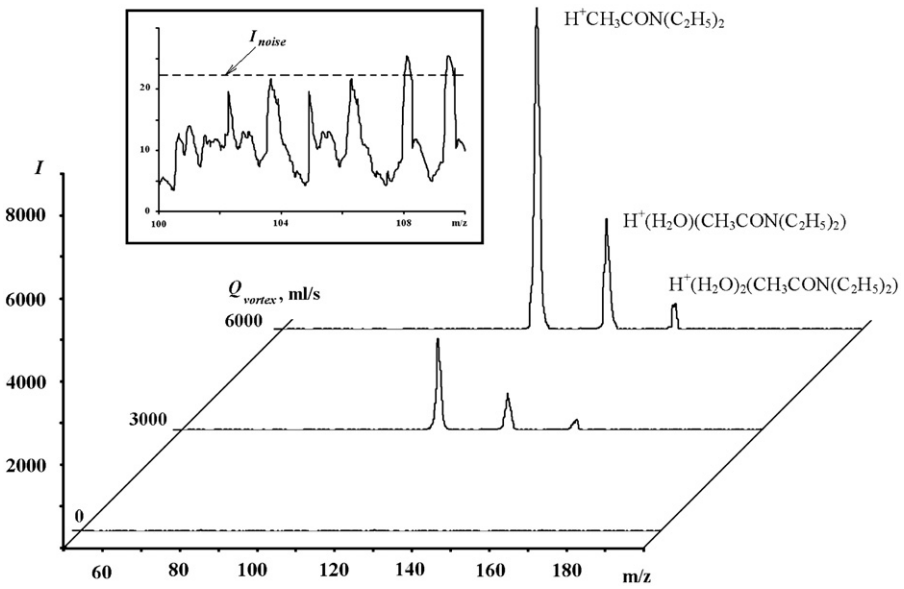

Fig. 4. Mass-spectra of *N*,*N*-diethylacetamid—$CH_3CON(C_2H_5)_2$ for different values of vortex flow, Q_{vortex}. The inset gives a noise level within the range of 100–110 m/z and a calculated noise level, I_{noise} (dashed line) for this range Additional flow, $Q_{add}=3800$ ml/s. The plate is covered with grid 2. The distance between the reflector and plate, $L=1$ cm.

spectrum. The intensity of mass-spectrometric peaks decreases as the distance between the plate and the sampling opening increases. This will be discussed below.

It should be mentioned that vortex (Q_{vortex}) and additional (Q_{add}) flows affect significantly the value of the peaks in resulting mass-spectra. Fig. 4 gives mass-spectra of *N*,*N*-diethylacetamid—$CH_3CON(C_2H_5)_2$ (protonated molecular ion and its water clusters) for different values of Q_{vortex}, with constant additional flow $Q_{add}=3800$ ml/s. As evident from Fig.4, noise alone is registered with $Q_{vortex}=0$. Peaks of diethylacetamid and its water clusters appear with $Q_{vortex}=3000$ ml/s and increase considerably with $Q_{vortex}=6000$ ml/s. We normalized the intensity of the registered peaks to the noise level to evaluate the resulting mass-spectra. An inset of Fig. 4 gives noise in a mass range of 100–110 m/z (that is in immediate vicinity of the normalizable peak of protonated diethylacetamid −116 m/z). We calculated the noise level by formula $I_{noise}=2\Sigma I_i/N$, where I_i is the noise level at a digitized point and N is a number of points. We took the summation over all the points of the chosen range (MC gives positive values of I_i). In the inset of Fig.4 I_{noise} is given by a dashed line. In should be mentioned that the noise level is somewhat increased when the additional and vortex flows are fed, most likely this is due to the appearance of a chemical component in noise.

To choose the operating values of the vortex and additional flows, we determined the dependencies $I/I_{noise}(Q_{vortex})$ (Fig. 5) and $I/I_{noise}(Q_{add})$ (Fig. 6) for the ions of different compounds.

As Figs. 5 and 6 suggest the MS signal from all compounds increases with Q_{vortex} and Q_{add} flows, for which a buildup of a reduced pressure at the vortex stream axis and an increase in the intensity of the composite vortex core produced by the vortex forming device are responsible. Reducing the pressure increases the number of ions pulled through the plate grid into the counter vortex flow. And an increase in the intensity of the composite vortex core enhances the efficiency of sample ion focusing towards the stream axis owing to a considerable increase of the radial velocity component. It seems likely that saturation of the MS signal registered from the ions of aniline is due to a balance of two processes: on one hand, enhancement of focusing and sample ion pull through the grid; on the other hand, prevention of the ion

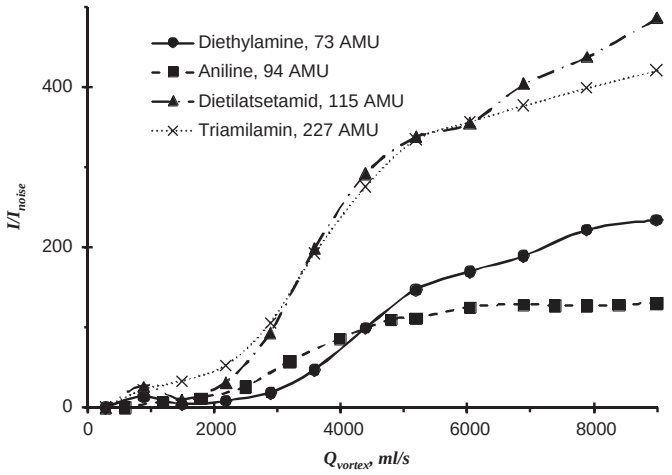

Fig. 5. Curve of the MS signal from protonated molecular ions versus vortex flow. Additional flow, $Q_{add}=3800$ ml/s. The plate is covered with grid 2. Distance between the reflector and plate, $L=1$ cm.

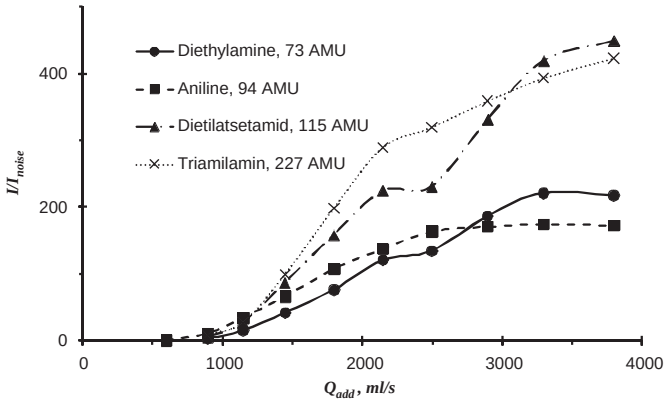

Fig. 6. Curve of the MS signal from protonated molecular ions versus additional flow. Vortex flow, $Q_{vortex}=9000$ ml/s. The plate is covered with grid 2. Distance between the reflector and plate, $L=1$ cm.

transportation to the mass-spectrometer with a field barrier is produced by the potential of the MS sampling capillary. Aniline is a rather light and the most compact molecule among the tested ones which features a high mobility in air—2.07 $sm^2/(V\,s)$ [24,25] and therefore a greater effect of electric field on it. We think that this explains the entrance of $I/I_{noise}(Q)$ dependence into saturation, for aniline first.

As a vortex forming device for further investigation we have chosen – by results of experiments – a device with a plate which opening is covered with the grid and operating values of the vortex and additional flows are $Q_{vortex}=9000$ ml/s and $Q_{add}=3800$ ml/s. We have chosen operating values of the vortex and additional flows and the right vortex forming device design going from the maximum values of the registered MS signals.

3.2. Research on the remote vortex stream efficiency upon positive ion sampling

To evaluate the efficiency of the remote vortex sampling, we determined the MS signal from positive ions versus distance, L, between the reflector and the plate of the vortex forming device with $Q_{vortex}=9000$ ml/s and $Q_{add}=3800$ ml/s. The sample source (the opening in the plate covered with the grid) was positioned at the sampler axis. Fig. 7 gives the measurement results in relative units. The MS signal from positive reactant ions versus the distance upon ionization by the ^{63}Ni source (curve 1) described in [19] is shown for comparison in the inset. Due to different dimensions of the compared vortex forming devices, the distance dependence of the MS signal is expressed in relative units from the relation L/D, where D is the reflector diameter.

As Fig. 7 suggests a considerable drop in the registered signal for all compounds tested is observed with the growth of the distance between the plate and reflector. Thus, at distance $L/D=0.4$ the MS signal reduces by more than an order of magnitude. For comparison, only a threefold decrease (curve 1 in the inset) is registered for the signal from the ^{63}Ni source with $L/D=0.4$. We think that such a difference is attributed to a strong effect of the field barrier between the plate and MS inlet capillary (Fig. 2, curve 7) on the process of ion focusing. In the experiments with ^{63}Ni (Fig. 7, curve 1 of the inset) the field barrier is missing, and the signal drop results from the recombination processes (^{63}Ni produces bipolar plasma) and the action of the volume charge. In our case of the corona discharge usage plasma is unipolar; and, on the one hand, the effect of the volume charge increases and, on the other hand, the action of the field barrier is

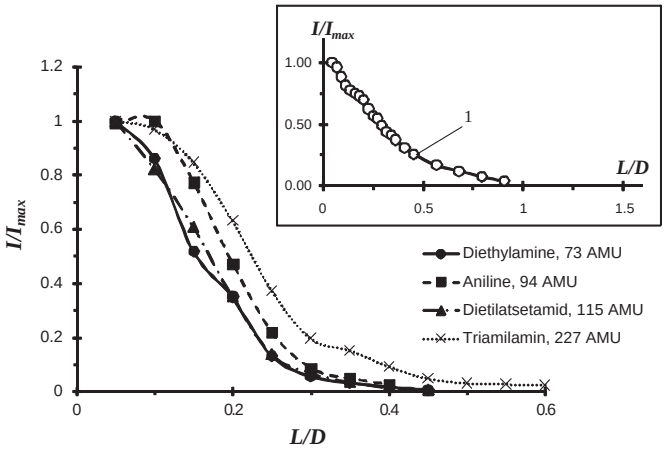

Fig. 7. Curve of the MS signal versus distance between the reflector and the plate of the vortex forming device. 1—signal from positive reactant ions from the ^{63}Ni [19] radioactive source and D—diameter of the vortex forming device reflector.

added. These two factors offer a strong dependence of the MS signal on distance, L/D, yielding a 2 times decrease in the efficiency of the remote vortex transportation.

Neutral species are also produced in the corona discharge. These species are trapped by the vortex flow and can interact with positive ions during their motion in the counter flow affecting the efficiency of focusing and relative content of positive ions entering the inlet opening of the MS. Ozone and nitrogen oxides are usually produced in air of the corona discharge [26]. We have found no additional peaks in mass-spectra that correspond to the products of the ion interaction with these compounds, for example, the products of the target compound oxidation with ozone molecules. But this does not mean that such an interaction does not occur, since molecules with a low proton affinity may be produced as a result. But this problem requires additional study and will be the goal of our further research.

It is important to note some difference in the efficiency of the remote vortex focusing for different compounds comparing the $I/I_{max}(L/D)$ dependencies. Thus, the highest signal drop is observed for the smallest ion, diethylamine, 73 AMU. Triamilamin – a compound with the largest molecular weight, 227 AMU – shows the highest focusing efficiency. The difference in the focusing efficiency may be attributed to different values of the ion mobility of these compounds. As a rule, the higher is ionic mass the lower is its mobility. And hence, heavier ions are less subject to the action of the electric fields of the field barrier. The $I/I_{max}(L/D)$ dependence for the ion of dietilatsetamid, 115 AMU falls out of this rule. Dietlilatsetamid features the same strong signal drop with a distance as diethylamine—a compound with the lowest molecular weight of 73 AMU. This may result from the peculiarities of the molecule composition in which oxygen affecting the coefficient of its mobility is present.

3.3. Research on the efficiency of positive ion sampling with the vortex stream

To evaluate the efficiency of positive ion sampling, we determined the MS signal versus the value of the ionization source displacement from the sampler axis. As is given in [19], the radial velocity in the region of the vortex stream counter flow directed towards the stream axis allows the use of the vortex flow for a "gas-dynamic" ionized sample focusing. It is of interest thereby to see how the field barrier between the plate and MS inlet capillary affects the efficiency of ion sampling.

Fig. 8 gives the MS signal relative to a maximum versus the displacement of the protonated aniline ion source about the axis of the vortex forming device for distances $L/D=0.1$ (1) and $L/D=0.3$ (2). The signal dependence (3) for positive reactant ions of the ^{63}Ni source from [19] is given for comparison. The source is displaced at right angle to the sampler axis. A value of the ion source displacement from the device axis is expressed in relative units against the radius of the vortex forming device reflector, (x/R) to avoid the action of absolute dimensions of devices used.

As Fig. 8 suggests three dependencies have a maximum at the vortex stream axis and decrease as they diverge from it. The nature of the experimental point distribution is well described by a Gaussian function and is shown by lines in Fig. 8. The narrowest distribution described by a Gaussian curve (Fig. 8, solid line) with $\sigma=0.08$ (σ—root-mean-square deviation) corresponds to the MS signal dependence determined for the ions of aniline with $L/D=0.1$ (1). For this dependence, displacement of the ion source from the vortex stream axis by a distance of $x/R=0.2$ yields a 13 times decrease in the signal from aniline ions. Distribution of registered signals spreads with the distance between the plate and ion source. Thus, the distribution of MS signals for aniline ion with $L/D=0.3$ (2) is approximated by a Gaussian function with $\sigma=0.12$ (Fig. 8, dashed line), and at a distance of $x/R=0.2$ the signal

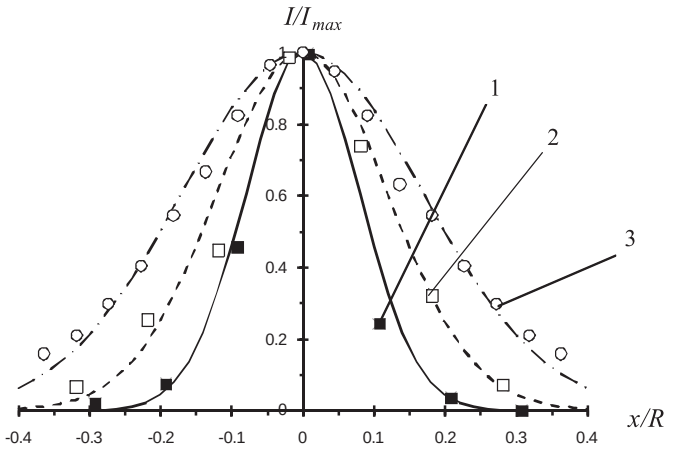

Fig. 8. Curve of the MS signal versus ion source displacement relative to the vortex sampling axis. 1—protonated ion of aniline $H^+(H_2NC_6H_5)$ (corona discharge, distance between the plate and reflector, $L/D=0.1$, the opening in the plate is covered with grid 2), 2—protonated ion of aniline $H^+(H_2NC_6H_5)$ (corona discharge; distance between the plate and reflector, $L/D=0.3$; the opening in the plate is covered with grid 1), and 3—signal for positive reactant ions from the ^{63}Ni radioactive source [19] (distance between the plate and reflector, $L/D=0.34$).

undergoes a four times reduction. Such a spread of the signal distribution may be explained by an inherent strong spread of the vortex stream along the flow [14], which in its turn expands the region of the sample ion collection. One should not forget thereby about a sharp decrease of the registered signal, which has caused one to conduct experience with a coarser grid at distance $L/D=0.3$ to increase the amount of sample pulled through the plate.

The most wide spread of the registered signal (3) corresponds to positive reactant ions of the ^{63}Ni radioactive source. It is described by a Gaussian curve with $\sigma=0.17$ (Fig. 8 dot-and-dash curve), and at a distance of $x/R=0.2$ the registered signal undergoes a two and a half times reduction. Therewith, the distance between the plate and reflector is $L/D=0.34$ which is consistent with the distance for experimental points (2) in Fig. 8. Experimentally, an essential difference for curves (2) and (3) is the absence of the field barrier for (3). One may state based on the experimental data that the field barrier narrows considerably (more than one and a half) the region of the sample ion collection with the vortex stream.

It should be mentioned that the action of sheath flow, Q_{sheath}, within 200 ml/s gives a slight spread of the registered signal distribution of no more than 30%.

4. Conclusion

Investigations have shown a possibility to focus the ionized unipolar samples with the swirled vortex stream upon the corona discharge ionization and the field barrier present in the sampling region. It is shown that under certain conditions the use of the vortex stream and additional flow enhances the signal from the target ions in the mass-spectrum by more than two orders of magnitude with respect to noise. With the vortex flow total ion current quintuples as compared to a case when ions are introduced directly from the corona discharge with the plate, vortex stream and additional flow missing. The availability of the field barrier that causes considerable narrowing of the region of the ionized sample collection will call for a precise adjustment of the plate relative to the vortex flow.

Data on the ionized sampling efficiency obtained are of particular importance for analytical applications. The well-known techniques of the atmospheric pressure desorption/ionization (as DESI [27], DART [28] and others [29]) produce ions scattered over a large volume, and ions are sampled through a small capillary or an opening, which results in the loss of sensitivity. The use of the vortex focusing permits one to increase the amount of the ionized sample delivered to the mass-spectrometer and enhance the analysis sensitivity. The use of vortex ion focusing is equivalent to an increase of the inlet gas analyzer opening (in our case, the area of the sampling capillary opening of the mass-spectrometer $\sim$0.1 mm^2, the area of opening in the plate $\sim$100 mm^2). We will prove this idea in further experiments.

The main drawback of the suggested focusing technique for analytical chemistry applications is a high gas flow rate (4–9 l/s), and hence the use of noble gases (argon and helium) for the vortex steam formation is too costly. Even the use of pure nitrogen presents a problem, since with these flow rates one standard pure nitrogen cylinder will expend itself in 20 min. Nevertheless, there are many methods of desorption/ionization (for field applications) where air is used as a carrier-gas and a discharge gas. In these cases focusing with a highly swirled vortex stream may enhance the analysis sensitivity. The conditions (temperature, humidity, and additives) under which air creating a vortex flow is kept, the use of other gases for the vortex flow creation, and the effect thereof on the analysis efficiency are the subject of our further investigations.

Acknowledgments

The authors thank Dr. Stephan Barlow (NIST, Boulder, CO, USA) for helpful comments and help for proper English. This work is supported by the Presidium of the Russian Academy of Sciences, Program 9, Project 5 and the Russian Foundation for Basic Research (Grant no. 11-08-00329a).

References

[1] H. Kambara, I. Kanomata, Mass Spectrosc. 24 (1976) 229–236.
[2] E.P. Kremer, G.J. Evans, R.E. Jervis, J. Phys. D: Appl. Phys. 39 (2006) 5008–5015.
[3] S. Shaffer, K. Tang, G. Anderson, D. Prior, H. Udseth, R. Smith, Rapid Commun. Mass Spectrom. 11 (1997) 1813–1817.
[4] S. Shaffer, D. Prior, G. Anderson, H. Udseth, R.D. Smith, Anal. Chem. 70 (1998) 4111–4119.
[5] T. Kim, A. Tolmachev, R. Harkewicz, D. Prior, G. Anderson, H. Udseth, R. Smith, T. Bailey, S. Rakov, J. Futrell, Anal. Chem. 72 (2000) 2247–2255.
[6] B. Clowers, Y. Ibrahim, D. Prior, W. Danielson, M. Belov, R. Smith, Anal. Chem. 80 (3) (2008) 612–623.
[7] R. Guevremont, R.W. Purves, Rev. Sci. Instrum. 70 (1999) 1370–1383.
[8] R. Guevremont, L. Ding, B. Ells, D.A. Barnett, R.W. Purves, J. Am. Soc. Mass Spectrom 12 (2001) 1320–1330.
[9] D.A. Barnett, B. Ells, R. Guevremont, R.W. Purves, J. Am. Soc. Mass Spectrom. 13 (2002) 1282–1291.
[10] L. Zhou, B. Yue, D. Dearden, E. Lee, A. Rockwood, M. Lee, Anal. Chem. 75 (2003) 5978–5983.
[11] Hawkridge, L. Zhou, M. Lee, D. Muddiman, Anal. Chem. 76 (2004) 4118–4122.
[12] Hawkridge, D. Muddiman, Anal. Chem. 77 (2005) 6174–6183.
[13] R. Dixon, D. Muddiman, A. Hawkridge, A. Fedorov, J. Am. Soc. Mass Spectrom. 18 (2007) 1909–1913.
[14] In: R.B. Akhmedov (Ed.), Aerodynamics of Swirled Stream, "Energy", Moscow, 1977, p. 18 (in Russian).
[15] F.K. Rashidov, A.K. Sakaev, Proceedings of the IV Republican Scientific and Technical Energy Workshop, Tashkent, September 1973, pp. 108–109 (in Russian).
[16] Yu.N. Kolomiets, V.V. Pervukhin, Tech. Phys. Lett. 35 (17) (2009) 18–25.
[17] Yu.N. Kolomiets, V.V. Pervukhin, Talanta 81 (1–2) (2010) 294–300.
[18] Yu.N. Kolomiets, V.V. Pervukhin, Tech. Phys. Lett. 37 (5) (2011) 465–468.
[19] Yu.N. Kolomiets, V.V. Pervukhin, Talanta 85 (2011) 1792–1797.
[20] Yu.N. Kolomiets, Sorpt. Chromatogr. Processes 2 (5–6) (2002) 575–585 (in Russian).
[21] Thomas R. Covey, Bruce A. Thomson, Bradley B. Schneider, Mass Spectrom. Rev. 28 (2009) 870–897.
[22] V.V. Pervukhin, R.R. Ibragimov, V.M. Moralev, Instrum. Exp. Tech. 40 (5) (1997) 700–701.
[23] Yu.N. Kolomiets, Sorpt. Chromatogr. Processes 2 (5–6) (2002) 563–574. (in Russian).
[24] Z. Karpas, Z. Berant, J. Phys. Chem. 93 (1989) 3021–3025.
[25] W.E. Steiner, W.A. English, H.H. Hill, J. Phys. Chem. A 110 (2006) 1836–1844.